

THE FORMATION OF PRECIOUS OPAL: CLUES FROM THE OPALIZATION OF BONE

BENJAMATH PEWKLIANG, ALLAN PRING[§] AND JOËL BRUGGER

*Department of Mineralogy, South Australian Museum, North Terrace, Adelaide, South Australia 5000,
 and School of Earth & Environmental Sciences, Discipline of Geology & Geophysics,
 University of Adelaide, Adelaide 5005, South Australia, Australia*

ABSTRACT

The composition and microstructure of opalized saurian bones (Plesiosaur) from Andamooka, South Australia, have been analyzed and compared to saurian bones that have been partially replaced by magnesian calcite from the same geological formation, north of Coober Pedy, South Australia. Powder X-ray-diffraction analyses show that the opalized bones are composed of opal-AG and quartz. Major- and minor-element XRF analyses show that they are essentially pure SiO₂ (88.59 to 92.69 wt%), with minor amounts of Al₂O₃ (2.02 to 4.41 wt%) and H₂O (3.36 to 4.23 wt%). No traces of biogenic apatite remain after opalization. The opal is depleted in all trace elements relative to PAAS. During the formation of the opal, the coarser details of the bone microstructure have been preserved down to the level of the individual osteons (scale of around 100 μm), but the central canals and the boundary area have been enlarged and filled with chalcedony, which postdates opal formation. These chemical and microstructural features are consistent with the opalization process being a secondary replacement after partial replacement of the bone by magnesian calcite. They are also consistent with the opal forming first as a gel in the small cavities left by the osteons, and the individual opal spheres growing as they settle within the gel. Changes in the viscosity of the gel provide a ready explanation for the occurrence of color and patch banding in opals. The indication that opalization is a secondary process after calcification on the Australian opal fields is consistent with a Tertiary age for formation.

Keywords: opal, formation, gel, bone, fossilized, replacement, Australia.

SOMMAIRE

Nous avons analysé la composition et la microstructure d'ossements de sauriens (Plésiosaur) opalisés provenant de Andamooka, en Australie australe, et nous avons établi une comparaison avec des ossements de sauriens partiellement remplacés par la calcite magnésienne dans la même formation géologique au nord de Coober Pedy, également dans le sud de l'Australie. D'après les spectres de diffraction X, les os opalisés contiennent l'opale-AG et le quartz. Les compositions, en termes d'éléments majeurs et en traces, montrent qu'il s'agit de la silice presque pure (de 88.59 à 92.69%, poids), avec des quantités moindres de Al₂O₃ (entre 2.02 et 4.41%) et H₂O (entre 3.36 et 4.23%). Il n'y a aucune trace d'apatite biogénique suite à l'opalisation. L'opale est dépourvue de tous les éléments traces par rapport avec l'étalon PAAS. Au cours de la formation de l'opale, les détails les plus grossiers de la microstructure des os ont été préservés jusqu'à l'échelle des ostéons individuels (environ 100 μm), mais les canaux centraux et les bordures ont été élargis et remplis de calcédoine, apparue après la formation de l'opale. D'après ces caractéristiques chimiques et microstructurales, l'opale résulterait d'un processus secondaire suite au remplacement partiel des os par la calcite magnésienne. L'opale se serait d'abord formée sous forme de gel dans les petites cavités laissées par les ostéons, et les sphères individuelles d'opale aurait cru au cours de leur tassement dans ce gel. Des changements dans la viscosité du gel seraient à l'origine des bandes de couleurs et de zones incolores dans l'opale. L'indication que la formation de l'opale est un processus secondaire développé après la calcification des champs opalifères australiens concorde avec un âge tertiaire de formation.

(Traduit par la Rédaction)

Mots-clés: opale, formation, gel, ossements, fossilisé, remplacement, Australie.

[§] E-mail address: pring.allan@saugov.sa.gov.au

INTRODUCTION

The process of mineralization of bone and shell for preservation in the fossil record is dependent on the chemical and physical conditions during diagenesis, particularly the composition of the mineralizing fluid. Fundamentally, these processes can be considered as mineral-replacement reactions, in which the biomineral is replaced by another mineral such as quartz, opal or calcite. The replacement reaction can also be associated with recrystallization of the biomineral, particularly biogenic apatite (carbonate-hydroxylapatite), during which trace amounts of heavy metals may be incorporated into the apatite structure (Hubert *et al.* 1996). For the very-fine-scale microstructure of the fossil to be preserved, the dissolution reaction that affects the biomineral and any soft tissue present must be tightly coupled to the precipitation reaction, so that little free space occurs at the reaction front (Putnis 2002). Such replacement reactions therefore proceed as the fluid fronts move through the fossil. If the dissolution and precipitation reactions are not tightly coupled and there is a gap between the dissolution front and the precipitation front, then the fine details of the microstructure will not be preserved.

We report here the results of a detailed investigation of the chemical composition, structure and microstructure of opalized marine reptile bones from Andamooka, South Australia. This material is compared to samples of fossilized bone of a marine reptile from near Coober Pedy that have not been opalized, and of a bone from a modern dolphin (*Delphinus delphis*). The aim of this study is to better understand the process of opal formation in the Australian Opal Fields, particularly the nucleation, growth and settling of the silica spheres. We aim to check whether opalization of the fossil bones could occur as a tightly coupled dissolution–precipitation reaction, or whether opal simply filled cavities resulting from the dissolution of the bone material. We published a preliminary version of this work as an extended abstract in a conference proceeding (Pewklian *et al.* 2004). We have since undertaken a detailed re-examination of the textural relationship between the minerals in the opalized bones and re-evaluated the evidence for the mechanism of opal formation. We no longer consider some of the conclusion reached in Pewklian *et al.* (2004) valid.

BACKGROUND INFORMATION

There are two types of opal: microcrystalline opal consists of opal-CT (tridymite) and opal-C (cristobalite), and non-crystalline opal consists of opal-A, opal-AN and opal-AG. Opal-A is a biogenic form of silica, opal-AN (“hyalite”) is a hydrous amorphous silica glass (Flörke *et al.* 1973), opal-AG is the form found in precious opal (which shows a play of colors)

and potch opal (which does not). Opal-AG is an ordered arrangement of spheres (1700 to 3500 Å in diameter) consisting of non-crystalline, amorphous, gel-like silica with H₂O filling the interstices (Jones *et al.* 1964). It is the ordered distribution of the uniformly sized spheres of silica that causes the play of colors seen in precious opal (Sanders 1964, Darragh *et al.* 1976). Both the microcrystalline and non-crystalline forms of opal contain variable amounts of non-essential H₂O but are otherwise usually pure, with contents of non-volatile impurities below 1 mol.% in most samples, and commonly below 0.5 mol.% (Graetsch 1994, McOrist & Smallwood 1995, 1997, McOrist *et al.* 1994, Brown *et al.* 2004).

Williams *et al.* (1985) and Williams & Crerar (1985) gave a comprehensive review of the diagenesis of silica and the physical and chemical controls on the formation of the various forms of silica, including opal. They noted that opal-A is the most soluble form of silica and that quartz is the least soluble, that opal-A is generally the first polymorph to form, and that it can readily transform *via* dissolution–precipitation reactions to opal-CT and on to quartz. They concluded that authigenic precipitation of high-silica clays or zeolites could conceivably remove silica from solution rapidly enough to cause the steady-state concentrations of dissolved silica to fall below the quartz-solubility curve. But they noted that growth of opal-A over quartz, the thermodynamically stable form, is likely to be due to the polymerization of silica in solution. Iler (1979) reported that the polymerization of silica into three-dimensional gel-like networks is favored in the pH range 3 to 10 where dissolved salts are present in solution, as the polyvalent cations in solutions overcome the mutual repulsion of the silica colloids, which have negatively charged surfaces. Williams & Crerar (1985) concluded that four factors in addition to the morphology and structure of the silica polymorph control the concentrations of silica in pore waters in sediments. These are: pH, temperature, type of species of dissolved silica, and the presence of additional minerals.

The geology of the Australian opal fields, which produce 95% of the world’s precious opal, has been studied in considerable detail (Jones & Segnit 1966, Carr *et al.* 1979, Robertson & Scott 1990, Barnes *et al.* 1992). However, there is still debate about the factors controlling, and the process leading to, the formation of precious opal and the “opalization” of fossils. In particular, there is considerable debate about the age of the opal, the source of the silica, the composition of the opalizing fluids, and the mechanism of formation of precious opal; see Barnes *et al.* (1992) and Horton (2002) for overviews. In many parts of the world, opal, including precious opal, is formed from volcanogenic fluids. Indeed, opal is a very common phase resulting from hydrothermal alteration of felsic volcanic rocks by acid sulfate fluids and from the boiling and mixing of

neutral chloride geothermal brines in epithermal settings (Corbett & Leach 1998). Brown & Bacon (2000) showed how it is possible to obtain industrial-grade uniformly sized (mono-dispersed) silica sols (100 to 700 Å in diameter) by cooling geothermal brines from the Wairakei geothermal field, New Zealand, under controlled conditions. In contrast, Australia's precious opal occurs in veins and nodules within bentonite clay layers in shales and sandstones, and has no direct link to magmatic activity (*i.e.*, it is "sedimentary" opal). Precious and potch opal are also found replacing shells, wood and, less commonly, the bones and teeth of marine reptiles (Barnes *et al.* 1992). The skeletons of Cretaceous plesiosaurs and ichthyosaurs that have been partially or completely opalized have been found at Andamooka, Coober Pedy and White Cliffs, Australia (Fig. 1) (Etheridge 1897, Kear 2003).

The two major models for opal formation in the Australian Opal Fields are: the deep weathering model (*e.g.*, Jones & Segnit 1966, Darragh *et al.* 1976, Kalinin & Serdobintseva 2003) and the syntectonic model (*e.g.*, Pecover 1996, see also Townsend 2007). In the former, opal forms slowly by downward percolation and interaction of meteoric water with rock in an arid to semi-arid environment. In contrast, the syntectonic model involves rapid formation of opal during hydraulic extension-related fracturing by silica-rich fluids under pressure. The latter model explains the location of the

major opal fields along the rim of the Great Artesian Basin (see Fig. 2) as a result of the hydrodynamics of the Great Artesian aquifer. Recently, Rondeau *et al.* (2004) re-examined the origin of Hungarian opal from the Červenica–Dubník region, now in Slovakia, which has long been attributed a volcanic origin. They found that the physical properties of the opal were those of opal-A (Jones & Segnit 1971) and thus similar to the sedimentary opal found in Australia. Their preliminary oxygen isotope measurements for both "Hungarian" and Australian opal from Coober Pedy gave a temperature of formation lower than 45°C compared to a temperature of 190°C for Mexican opal-CT of volcanic origin. These results are consistent with the deep weathering model rather than the syntectonic model.

It is worth noting that silicified micro-organisms are associated in a broad sense with opal (Dowell & Mavrogenes 2004), even though the role of biogenic activity in opal formation remains unknown. Were they simply present during opal formation, playing a passive role, for example in acting as centers of nucleation for silica precipitation or, alternatively, were they a necessary requirement for the geochemical environment to form opal? These silicified tests from micro-organisms are widespread in nature; Williams *et al.* (1985) discussed the dissolution of these tests in sedimentary environments and the deposition of opal-A and its subsequent transformation to opal-CT and quartz.

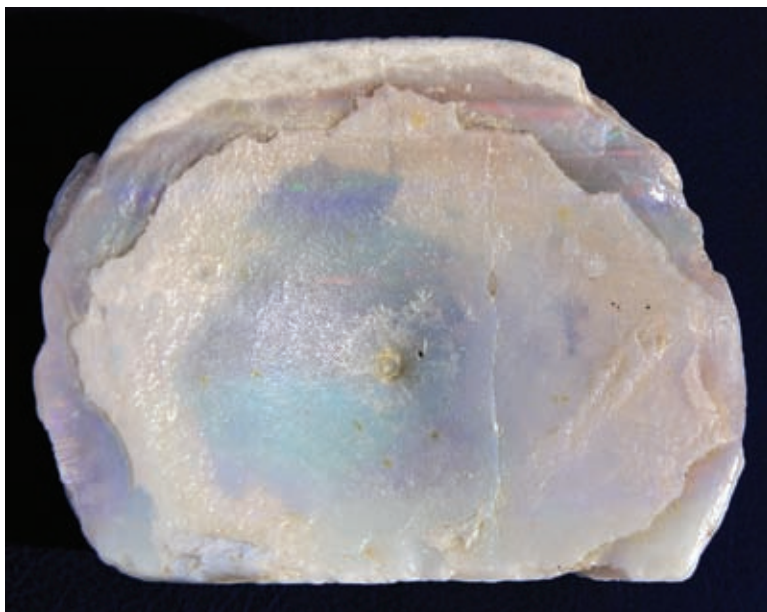


FIG. 1. Opalized vertebra from ichthyosaur *Platypterygins longmani* from the Bulldog shale, Coober Pedy, South Australia (on loan to the South Australian Museum). The vertebra is 5.8 cm across. Note the horizontal color-banding in the opal.

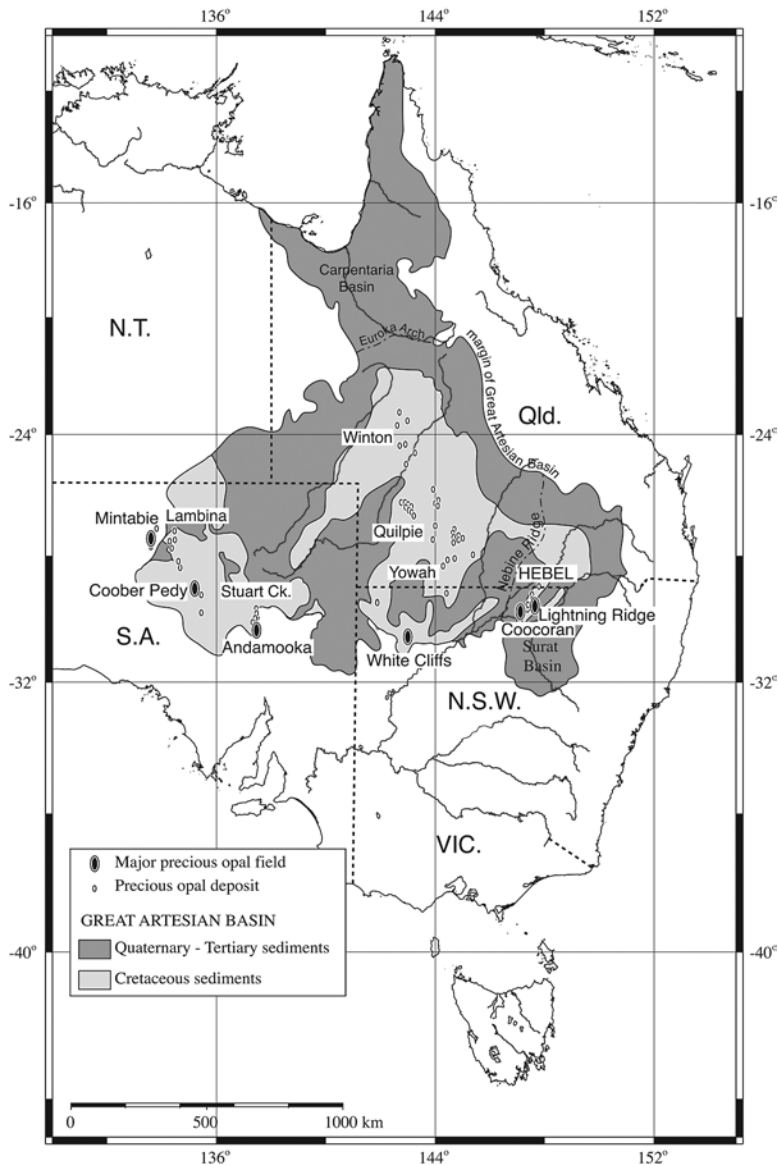


FIG. 2. Map showing the location of the principal of opal fields in relation to the Great Artesian Basin, modified after Habermehl (1980).

GEOLOGY OF THE SOUTH AUSTRALIAN OPAL FIELDS

The opalized fossils at Cooper Pedy and Andamooka, South Australia, are found within the opal-bearing layers of the Cretaceous Bulldog Shale (Barremian to Early Albian), whereas at White Cliffs, they are found within the Doncaster Member of the Lower Cretaceous Wallumbilla Formation (Late Barremian to Aptian;

Barnes *et al.* 1992, Horton 2002). Where fresh, the Bulldog Shale is a dark grey, silty and sandy, smectite-rich claystone with lenses of sand, limestone and occasional erratic boulders. Unopalized ichthyosaur bones have been found in beds of fresh Bulldog shale at Moon Plain some 60 km north of Cooper Pedy. In contrast, opal is found in weathered Bulldog shale consisting of bleached, porous, kaolinite-rich claystone overlying

darker, denser, smectite-rich claystone (Robertson & Scott 1990). This is believed to be caused by leaching of Cretaceous rocks during the Tertiary. Both precious and potch opal are found in the weathered Bulldog Shale as veins, infilling cracks and joints, occasionally replacing fossils within bentonite layers. Color banding is in some cases observed across opal masses, including opalized bones (Fig. 1). The stratigraphy and geology of the Andamooka and Coober Pedy fields are similar, and opal is commonly found as horizontal beds known as the opal level (Jones & Segnit 1966, Carr *et al.* 1979, Robinson & Scott 1990). Opal occurs on the surface down to a depth of about 40 m.

The age of the opal deposition remains controversial, mainly owing to the difficulties in dating opal itself. Recent attempts to date Australian precious opal using the U–Pb geochronometer were unsuccessful owing to its low U contents and high concentrations of common Pb (Amelin & Back 2006). Dating of black opal from Lightning Ridge with ^{14}C reveals Quaternary ages for the associated organic matter (Dowell & Mavrogenes 2004). However, most authors argue that opal formed during the Tertiary as a result of the weathering of the Bulldog shales (Darragh *et al.* 1966, Townsend 1976, Horton 2002). This view is supported by K–Ar dating of alunite associated with the transformation of the Bulldog shale to kaolinite, and also found in veins together with opal (Bird *et al.* 1990). In contrast, Barker (1980) and Pecover (1996) concluded that opalization occurred in the late Cretaceous and was more or less contemporaneous with the sedimentation.

THE MICROSTRUCTURE OF BONE

Bone consists of organic tissue and a mineral component, carbonate-hydroxylapatite, that forms as nanocrystals approximately 500 Å in length. Bone contains living cells within its structure and is continually modified during ontogeny. Numerous elongate cavities, called lacunae, host cells called osteocytes that are responsible for bone manufacture and resorption. Numerous small canals, the canaliculi, through which essential nutrients are exchanged and transported, interconnect these cells. There are also larger canals or channels that run through the center of the osteons. This network of small and larger canals is also known as the Haversian system. The central canal is 100 to 200 µm in diameter (Fig. 3), but variations in diameter are related to the age of the osteon and its relative position within the bone. The organic matrix is largely fibrillar collagen, in the form of tropocollagen.

The plesiosaurs and ichthyosaurs of the Mesozoic Era had bone structures that are broadly analogous to those of modern marine mammals. In contrast to modern turtles or lizards, whose bone structure shows growth rings, the skeletal material of plesiosaurs and ichthyosaurs was more dynamic in nature, being slowly dissolved and relayed in a fashion similar to that in

marine mammals. By making the outer layers of their bones spongy and less dense, modern deep-diving mammals can enhance the strength needed to support the body while remaining fairly buoyant (Motani 2004). The same type of spongy layer also occurs in the bones of ichthyosaurs and plesiosaurs, creating lighter skeletons (Motani 2004). As in the case with dolphins, structural features such as the primary osteons and lacunae with adjoining canaliculi should be present in perfectly fossilized bones.

Although we are not aware of any studies on the opalization of bones, there have been studies of the silicification of dinosaur bones. For example, Hubert *et al.* (1996) found that during diagenetic silicification of Jurassic dinosaur bones, the biogenic apatite-group mineral was recrystallized and enriched with trace metals, but that the fine-scale structures of the Haversian system were well preserved.

SAMPLES AND METHOD USED

Polished thin sections and blocks of several of opalized plesiosaur bones from the Andamooka opal field, South Australia, were examined; three were selected for detailed analysis. In addition, samples of non-opalized ichthyosaur bones from near Coober Pedy and a rib of a modern dolphin (*Delphinus delphis*) also were studied. Details of the samples examined in this study are summarized in Table 1.

Powder X-ray-diffraction patterns of the samples were obtained using a Huber Imaging Plate Guinier Camera with $\text{CoK}\alpha_1$ radiation. The samples were imaged using a XL30 field-emission gun scanning electron microscope (SEM). To obtain SEM images of the individual spheres of silica in the opal, some of the polished blocks were etched in a solution of 10 M hydrofluoric acid for 30 seconds. Images of the carbon-coated samples were obtained by using both the back-scattered electron detector and a secondary electron detector at either 10 kV or 15 kV. Energy-dispersive spectroscopy (EDS) was used for purposes of mineral identification.

The bulk major- and trace-element compositions were measured using a PW 1480 X-ray fluorescence (XRF) spectrometer. A pressed powder disc was used for analysis of the material for trace elements, and a fused disc was used for major-element analysis. The fused disc was prepared by heating a mixture of powdered sample and borate flux in a platinum alloy crucible at a high temperature (950–1250°C). The discs were prepared by pressing the powdered sample with a boric acid binder.

MICROSTRUCTURE AND MINERALOGY

The microstructure of modern dolphin rib-bone is shown in Figure 3. The details of the Haversian system are clearly recognizable, including the primary osteons

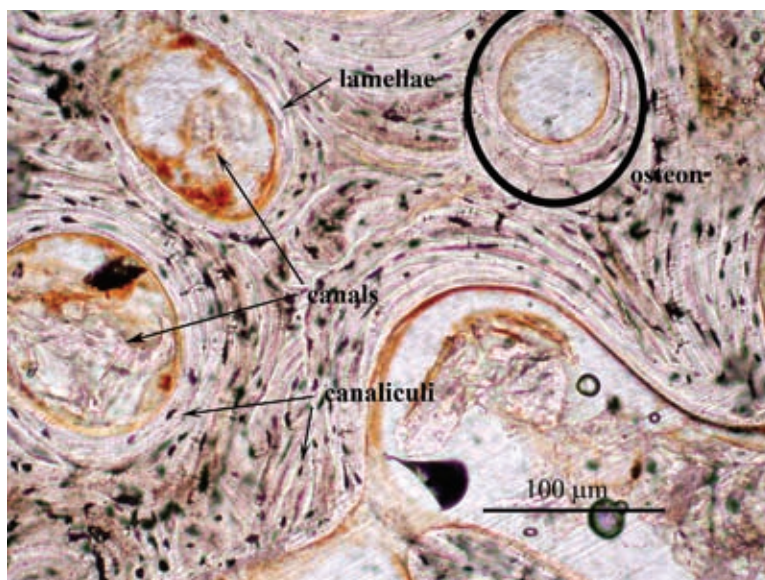


FIG. 3. Microtexture of rib bone from a modern dolphin (*Delphinus delphis*). The osteons, Haversian canals, canaliculi, and the lamellae of biogenic apatite and collagen are indicated.

TABLE 1. SUMMARY OF THE SAMPLES EXAMINED IN THE STUDY

Registration No.	Description	Locality
1 USNMNH ¹ 93815	Opalized wood	Columbia district, Nevada, USA
2 SAM ² M22204	Modern dolphin rib bone (<i>Delphinus delphi</i>)	Fowlers Bay, South Australia
3 SAM G31611	Fossilized Ichthyosaur limb (<i>Platypterygius longmani</i>)	Moon Plain, 40 km north of Coober Pedy, South Australia
4 SAM G31610	Opalized Plesiosaur rib or limb	Andamooka opal field, South Australia
5 SAM G31609	Opalized Plesiosauroidea rib	Andamooka opal field, South Australia
6 SAM G31612	Opalized Plesiosauroidea neural arch fragment	Andamooka opal field, South Australia

¹ U.S. National Museum of Natural History. ² South Australian Museum.

with the fibrous lamellae of the biogenic apatite and collagen, the canaliculi and the canals. The powder X-ray-diffraction pattern of the bone sample shows the characteristic broad reflections of carbonate-hydroxylapatite (Fig. 4).

The microstructure of the fossilized limb bone of an ichthyosaur from Moon Plain north of Coober Pedy is similar to that of the modern dolphin bone (Figs. 3, 5). The fibrous rings of biogenic apatite can just be seen along with the black canaliculi, although a carbonate mineral has replaced the collagen. The central canals appear slightly enlarged and are filled with a carbonate mineral that was identified by powder X-ray diffraction to be magnesian calcite. The boundaries between the

individual osteons may also be slightly enlarged and filled with magnesian calcite. Overall, the calcification of the bone has preserved details of the microstructure on a scale of micrometers (Fig. 5).

The X-ray-diffraction trace reveals that the reflections of biogenic apatite are somewhat sharper than in dolphin bone, indicating that the crystals of biogenic mineral have recrystallized during diagenesis. This diffraction trace is dominated by the sharp reflections of magnesian calcite, indicating partial replacement by this mineral (Fig. 4). The magnesian calcite fills the central canals of the osteons, surrounds their boundaries, and also impregnates the carbonate-hydroxylapatite in the osteon microstructure.

The microstructure of the opalized plesiosaur bone is recognizable as bone, and the shapes of the individual osteons are clearly visible. The central osteone canals and the boundary areas have been enlarged by a factor of at least two compared to modern dolphin bone, and no longer have smooth, sharply defined edges. These areas are filled by fibrous chalcedony, as are cracks connecting some of the canals to the boundary areas. The biogenic apatite has been completely replaced by opal, which has a somewhat cloudy appearance due to the inclusion of micrometric flakes of kaolin. The canaliculi have completely disappeared, as have the fibrous microstructure of the osteons. The scale of the microstructural details preserved is of the order of 100 to 200 μm (Fig. 6).

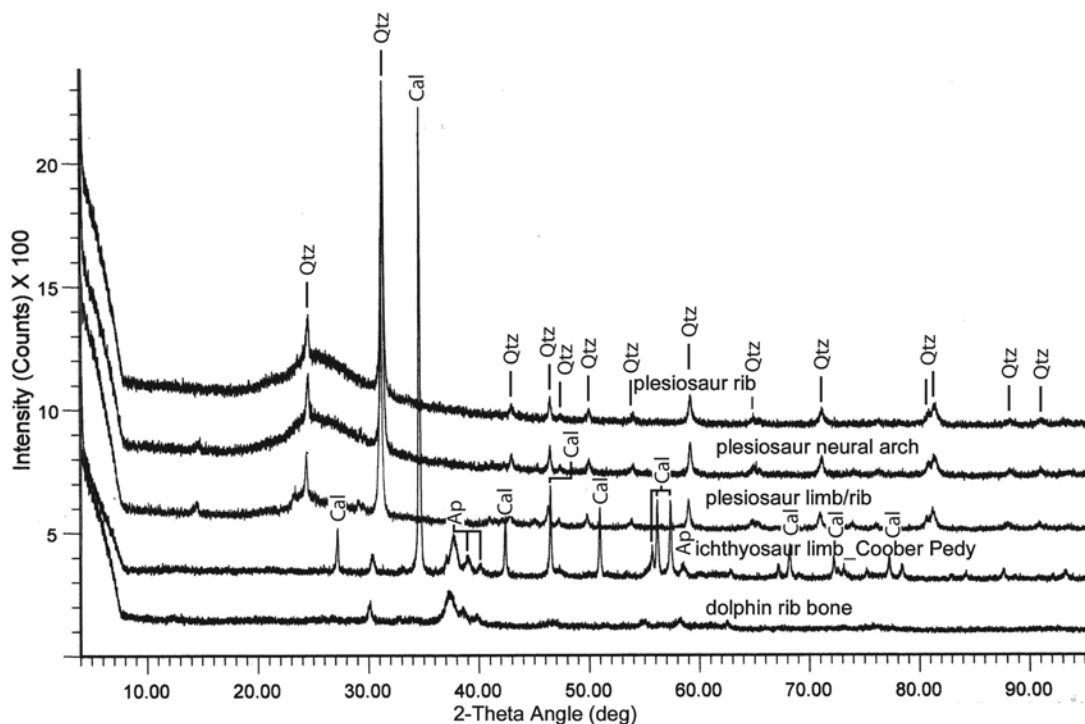


FIG. 4. X-ray-diffraction patterns of opalized and fossilized bones from plesiosaurs and ichthyosaurs and a pattern from a bone of a present-day dolphin.

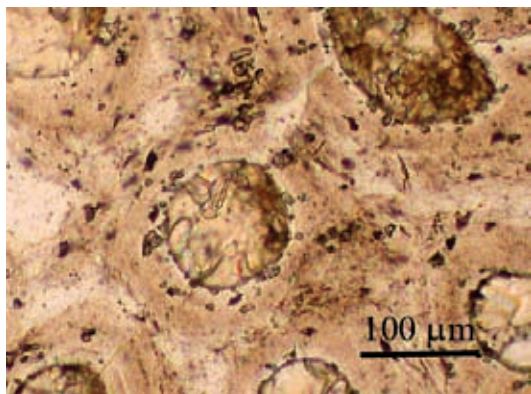


FIG. 5. Microtexture of a fossilized bone of an ichthyosaur from Moon Plain, north of Coober Pedy, South Australia. Note the degree of microstructural preservation, indicating a closely coupled replacement-reaction during fossilization.

The X-ray-diffraction patterns for the three opalized plesiosaur bones are all very similar and are dominated by the sharp reflections of quartz, due to the chalcedony filling the canals and the boundary cracks, and some alluvial quartz that has been washed into the larger cracks and cavities in the bone (Fig. 4). Note, however, the wide hump in the background between 2θ 22° and 30° , that is attributed to the amorphous structure of opal-AG (Jones & Segnit 1971).

CHEMICAL COMPOSITION OF MAJOR OXIDES AND TRACE ELEMENTS

The results of the major- and trace-element analysis of the samples are summarized in Table 2, together with results of previous trace-element analyses of precious opal by McOrist *et al.* (1994) and Brown *et al.* (2004). The opalized bones are essentially pure SiO_2 , with minor amounts of Al_2O_3 . The opalized bone samples contain no relict biogenic apatite. This is consistent with the bone structure having been completely recrystallized and replaced by opal and silica. In general, the trace-element profiles are similar to those reported by McOrist *et al.* (1994) and Brown *et al.* (2004), although

our results show elevated levels of Co. This may reflect contamination from the steel crusher used to pulverize the samples. Our samples also have elevated levels of Zr compared with the previously reported analysis. The Zr enrichment is probably due to traces of zircon in the sediments filling the larger channels in the bone structure. Robertson & Scott (1990) reported detrital zircon as a rare component of weathered Bulldog shale. The trace-element data, if normalized to the Post-Archean Australian Shale composite (PAAS), shows that the opal is depleted in all trace elements with the exception of Zr, which we attribute to detrital zircon (Taylor & McLennan 1985).

In contrast, the non-opalized bone of an ichthyosaur from Moon Plains (north of Coober Pedy) consists of biogenic apatite and high-Mg calcite, with only a small amount of silica. Trace-element data for the sample, when normalized to the PAAS composite, also show that the bone is depleted in all trace elements with the exception of a slight enrichment of Sr. The elevated

level of Sr is probably a product of the carbonate-rich mineralogy.

The trace-element patterns of the opalized samples of bone from Australian Opal fields can be contrasted with samples of opalized wood from Nevada (sample 1). The Nevada material is enriched in U, 48.1 ppm compared to 0.2 ppm, but like the opalized bone samples above, it is depleted in all other trace elements compared to PAAS. The bulk composition of modern dolphin bone consists of biogenic apatite with water and organic material, and their trace-element composition is broadly similar to that of the ichthyosaur bone from Moon Plain.

INTREPRETATION AND DISCUSSION

The Haversian system is preserved in the fossilized ichthyosaur bones, although the central canals and the boundary regions have increased in size during replacement by magnesian calcite. The carbonate-rich fluids

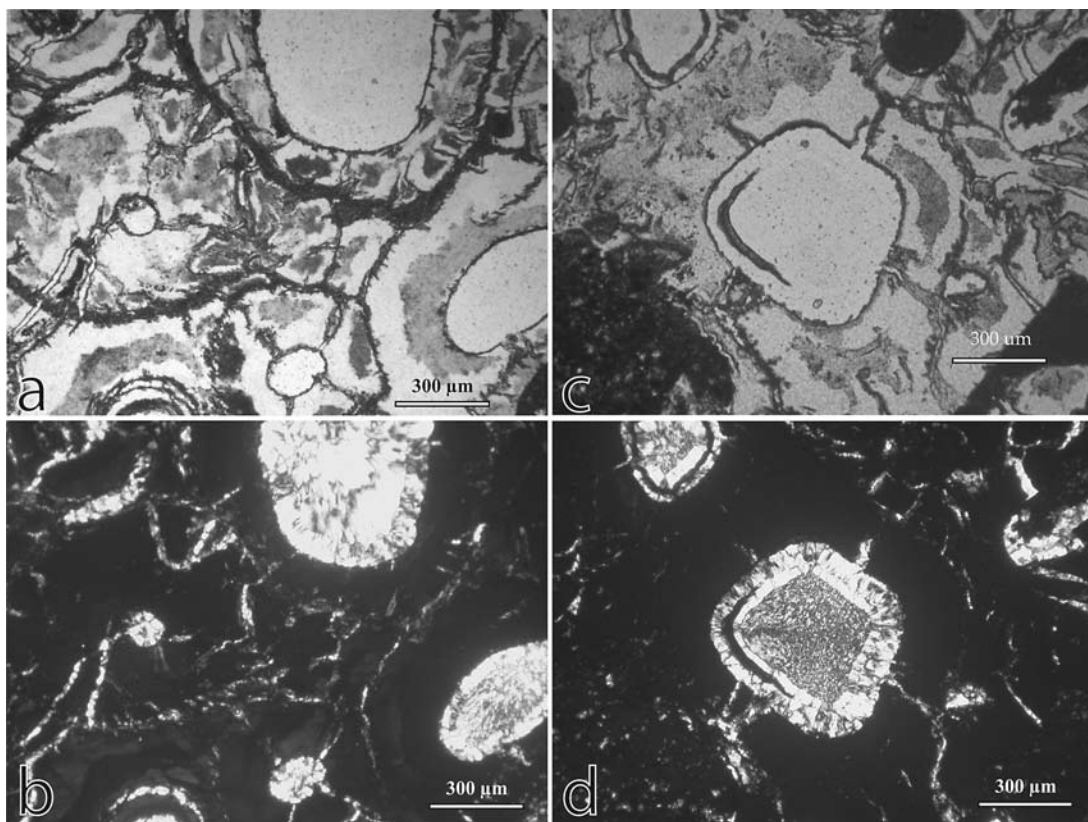


FIG. 6. Photomicrographs of the microstructure of opalized plesiosaur bone from Coober Pedy. Note that only the outlines of the osteons and the Haversian canals are preserved, not the fine microstructure as seen in the fossilized bone (Fig. 5). The canals and the spaces around the osteons are filled with chalcidony. Images a and c are taken in plane-polarized light, and images b and d are taken with crossed nicols.

TABLE 2. RESULTS OF THE MAJOR- AND TRACE-ELEMENT ANALYSES OF SELECTED SAMPLES

	opalized wood (1)	modern bone (2)	fossilized bone (3)	opalized bone (4)	opalized bone (5)	opalized bone (6)	McOrist <i>et al.</i> (1994)	Brown <i>et al.</i> (2004)
SiO ₂ wt%	84.58	0.15	2.27	91.87	88.59	92.69		
Al ₂ O ₃	0.26	0.04	0.76	2.12	4.41	2.02	6000 - 10000 ppm	
Fe ₂ O ₃ total	0.02	0.07	0.93	0.33	0.58	0.22	150 - 620	
MnO	0.01	0.01	0.59	0.01	0.01	0.01	4.2 - 14	8.3 - 94 ppm
TiO ₂	0	0.02	0.07	0.12	0.53	0.16		36 - 320
MgO	0.01	1.1	7.42	0.04	0.26	0.09	160 - 290	3.4 - 360
CaO	1.19	35.41	40.29	0.1	0.15	0.06	670 - 3100	2700 - 30000
Na ₂ O	0.26	0.77	0.61	0.31	0.36	0.28	280 - 1700	760 - 2300
K ₂ O	0.02	0.01	0.08	0.09	0.19	0.07	1000 - 3000	77 - 1200
P ₂ O ₅	0.01	26	12.3	0.01	0.01	0		
SO ₃	0.05	1.43	5.27	0.01	0	0.01		
LOI	13.78	31.88	26.99	4.16	4.23	3.63		
Total	100.18	96.88	97.57	99.16	99.3	99.23		
Sc ppm	1.3	0	0	1.3	3.4	1.1	0.04 - 0.4	
V	6	8	28	28	61	20		2.7 - 33
Cr	6	0	0	12	11	5		
Co	8	67	11	7	67	75	0.1 - 0.51	1.2 - 24
Ni	1	3	13	2	1	1		5.1 - 160
Cu	11	15	8	4	8	6		6.9 - 330
Zn	3	678	67	15	114	16		8.1 - 320
Ga	2.4	1.1	0.3	3.2	6.6	4.1		
Rb	1.1	0.5	4.9	10.9	15.3	8.8	11 - 23	
Sr	100.2	290.2	720.7	16.5	25.1	14.7	19 - 200	
Y	24.9	0	7	2.4	3.8	2.1		0.6 - 4.3
Zr	8.2	5.5	16.4	232.4	267.2	211.7		1.1 - 9.0
Nb	0.1	0	0	2.6	5.7	1.8		
Ba	18	6	204	259	236	248	140 - 490	
La	3	1	4	0	2	0	0.5 - 3.1	0.31 - 2.3
Ce	7	9	17	6	9	7	0.8 - 6.5	0.4 - 2.3
Nd	5	0	0	0	2	1		
Pb	0.4	1.6	0.4	2.6	1.6	2.6		
Th	2.4	2.7	0.7	1	1.3	1.9	0.05 - 1.7	
U	48.1	0.1	2	1.7	2.4	0.5		

thus moved through these openings during diagenesis and then permeated the ostonal structure, replacing the collagen and other organic material and recrystallizing the biogenic apatite. The X-ray-diffraction data indicate that the biogenic apatite was recrystallized during diagenesis, and the surrounding collagen and other organic material were replaced by carbonate. This micrometric-scale preservation of the bone structure indicates that the dissolution and replacement reactions were closely coupled. Finally, the canals and boundary veins were infilled with magnesian calcite. The enrichment in Sr suggests that this process took place in a marine environment, possibly shortly after burial.

In contrast, the opalized bones only show outlines of the Haversian system. The canals and boundary veins are greatly enlarged, have irregular edges and are filled with fibrous chalcedony. The chalcedony clearly post-dates opal deposition, as it fills cracks and surrounds small slithers of opal at the edges of the canals (Fig. 6). The opal has completely replaced the osteon structure, leaving no trace of the biogenic apatite or the fibrous microstructure. The reactions that led to the dissolution of the biogenic apatite and the precipitation of the opal

thus were probably not tightly coupled, and the opal precipitated in free space. Moreover, the cracks around the osteon boundaries and from the central canals indicate that the opal has contracted as it solidified. No sample of fossil bone that was only partially replaced with opal and carbonate could be found, despite an extensive search in the South Australian Museum's collections. All saurian bones were completely replaced by carbonate or by opal.

The nature of the preservation of the bone microstructure raises a number of questions about the formation of the opal. From the structural detail, we contend that the opal did not fill an open cast of the bone within the sediments. The fact that the boundary cracks and the canals are preserved and became enlarged suggests that these were already filled with a mineral before opalization took place. The mineral was later replaced by chalcedony after the opal had solidified, possibly as the result of a change in the pH of the groundwater or movements in the water table.

On the basis of this textural evidence, we can formulate the following hypothesis for the opalization of saurian bones at Andamooka, in terms of a

four-stage process: (i) diagenetic fossilization of the bones in a way similar to those still preserved at Moon Plain, with recrystallization of the biogenic apatite and infill of the Havesian system by a carbonate mineral; (ii) dissolution of the biogenic apatite, creating small (~100 µm) cavities in which opal and kaolinite are later deposited; (iii) dissolution of the carbonate, and (iv) precipitation of chalcedony in canals and cracks. Events (iii) and (iv) seem to have been coupled, and may have been promoted by the shrinkage resulting from opal "solidification"; this could have promoted fluid flow into the fossil bone. The microstructure of the chalcedony clearly shows a number of episodes of deposition (Figs. 6b, d). This four-stage scenario supports a post-Cretaceous timing for the opalization. The change in fluid composition required to destabilize the apatite and carbonate minerals that formed during diagenesis may have been brought about either by the deep weathering of the Bulldog shale in the Tertiary, or by the onset of the groundwater flow in the Great Artesian Basin.

How did the opal form? Were the opal spheres formed from solution in the sediment profile and washed down to fill into cavities in the bone, as Kalinin & Serdobintseva (2003) suggested, or did the opal spheres nucleate within the cavities or perhaps nucleate in the sediment profile and then continue to grow in osteon cavities? Darragh *et al.* (1976) noted that for the spheres to form, it was essential that they persist as free units, held in suspension by Brownian motion until they finally arranged themselves into an ordered accumulation of similarly sized spheres. Darragh *et al.* (1976) also suggested that the tiny spheres would settle very slowly in water; in a more viscous medium, like a gel, the time required for the spheres to settle down could be enormously long. The amount of free space in some of the smaller osteon cavities is around 100 µm, corresponding to the diameter of around 500 opal spheres. The evidence of shrinkage in the osteon-filling opal strongly suggests to us that the growth of the opal spheres took place within a silica gel that filled the network of osteons. The opal spheres grew as they slowly settled in the gel, possibly by a process of Ostwald ripening, as has been suggested by Williams & Crerar (1985). This could lead to the concentric rings observed in the TEM images of cross sections of spheres (see Darragh *et al.* 1976). Changes in the viscosity of the gel, resulting from oscillations in the level of the water table, from variations in climate or simply from changes in the gel composition as the spheres settle, would result in different periods of growth of the spheres, thus providing a ready explanation for the layering observed in some opalized bone and opal (Fig. 1). The proposal that the opal spheres grow in a gel is also supported by the presence of monomineralic, well-crystallized authigenic crystals of kaolinite, as a greater diversity of clay minerals and of morphologies would be expected if this kaolinite represented a detrital

component picked up by the opal-forming fluid. Note that this process does not totally preclude the possibility that nucleation of opal was initiated in the sediment profile. But it seems likely to us that if the silica spheres were formed in the profile, they must have been gel-like and contained some water, and they must have dried out during solidification, causing the shrinkage observed in the microstructure.

ACKNOWLEDGEMENTS

We thank Dr. Benjamin Kear, from the South Australian Museum, who helped select samples from the Museum collection and who provided advice on the taphonomy of the marine reptiles. Wally Fander provided expert assistance in the optical examination of the thin sections, Dr. Cristiana Ciobanu made many constructive comments on earlier drafts of this paper, and Dr. Catherine Skinner provided guidance in understanding the nature of bone. We also thank the staff of Adelaide Microscopy, especially Angus Netting, for assistance on the electron microprobe and the scanning electron microscope. Also, John Stanley and David Bruce at the Department of Geology and Geophysics, University of Adelaide, provided assistance in preparing samples for XRF analysis and HF etching. Dr. Pete Dunn of the U.S. National Museum of Natural History provided samples of opalized wood examined in this study. The thoughtful comments and editorial work of Dr. Carl A. Francis, Professor Robert F. Martin, and the two referees, Drs. Simon Pecover and Farrish Jenkins, have greatly improved the manuscript.

REFERENCES

- AMELIN, Y. & BACK, M. (2006): Opal as a U–Pb geochronometer: search for a standard. *Chem. Geol.* **232**, 67–86.
- BARKER, I.C. (1980): *Geology of the Coober Pedy Opal Fields with Special Reference to the Precious Opal Deposits*. M.Sc thesis, University of Adelaide, Adelaide, Australia.
- BARNES, L.C., TOWNSEND, I.J., ROBERTSON, R.S. & SCOTT, D.C. (1992): *Opal: South Australia's Gemstone*. South Australia Department of Mines and Energy, Adelaide, Australia (Handbook 5).
- BIRD, M.I., CHIVAS, A.R. & MCDUGALL, I. (1990): An isotopic study of surficial alunite in Australia. 2. Potassium–argon geochronology. *Chem. Geol.* **80**, 133–146.
- BROWN, K.L. & BACON, L. (2000): Manufacture of silica sols from separated geothermal water. Proc. World Geothermal Congress (Kyushu-Tohoku), 533–537.
- BROWN, L.D., RAY, A.S. & THOMAS, P.S. (2004): Elemental analysis of Australian amorphous banded opals by laser-ablation ICP–MS. *Neues Jahrb Mineral., Monatsh.*, 411–424.

- CARR, S.G., OLLIVER, J.G., CONOR, C.H.H. & SCOTT, D.C. (1979): Andamooka opal fields: the geology of the precious stone field and the results of the subsidised mining program. *Geol. Surv. South Aust., Rep. Invest.* **51**.
- CORBETT, G.J. & LEACH, T.M. (1998): Southwest Pacific gold-copper systems: structure, alteration, and mineralization. *Soc. Econ. Geol., Spec. Publ.* **6**.
- DARRAGH, P.J., GASKIN, A.J. & SANDERS, J.V. (1976): Opals. *Scientific American* **264**, 84-95.
- DARRAGH, P.J., GASKIN, A.J., TERRELL, B.C. & SANDERS, J.V. (1966): Origin of precious opal. *Nature* **209**, 13-16.
- DOWELL, K. & MAVROGENES, J. (2004): Black opal. *Geol. Soc. Aust., Abstr.* **73**, 68.
- ETHERIDGE, R. (1897): An Australian sauropterygian (*Cimoliasaurus*) converted into precious opal. *Rec. Aust. Mus.* **3**, 19-29.
- FLÖRKE, O.W., JONES, J.B. & SEGNI, E.R. (1973): The genesis of hyalite. *Neues Jahrb. Geol. Paläont., Monatsh.*, 82-89.
- GRAETSCH, H.I. (1994): Structural characteristics of opaline and microcrystalline silica minerals. In *Silica: Physical Behavior, Geochemistry and Materials Applications* (P.J. Heaney, C.T. Prewitt & G.V. Gibbs, eds.). *Rev. Mineral.* **29**, 209-232.
- HABERMEHL, R. (1980): The Great Artesian Basin, Australia. *J. Aust. Geol. Geophys.* **5**, 9-38.
- HORTON, D. (2002): Australian sedimentary opal – why is Australia unique? *Aust. Gemmol.* **21**, 287-294.
- HUBERT, J.K., PANISH, P.T., CHURE, D.J. & PROSTAK, K.S. (1996): Chemistry, microstructure, petrology, and diagenetic model of Jurassic dinosaur bones, Dinosaur National Monument, Utah. *J. Sedim. Res.* **66**, 531-547.
- ILER, R.K. (1979): *Chemistry of Silica*. Wiley-Interscience, New York, N.Y.
- JONES, J.B., SANDERS, J.V. & SEGNI, E.R. (1964): Structure of opal. *Nature* **204**, 990-991.
- JONES, J.B. & SEGNI, E.R. (1966): The occurrence and formation of opal at Coober Pedy and Andamooka. *Aust. J. Sci.* **29**, 129-133.
- JONES, J.B. & SEGNI, E.R. (1971): The nature of opal. I. Nomenclature and constituent phases. *J. Geol. Soc. Aust.* **18**, 57-68.
- KALININ, D.V. & SERDOBINTSEVA, V.V. (2003): Deposits of precious opal: genesis and search criteria. *Russ. Geol. Geophys.* **44**, 331-337.
- KEAR, B.P. (2003): Cretaceous marine reptiles of Australia: a review of taxonomy and distribution. *Cretaceous Res.* **24**, 277-303.
- MCORIST, G.D. & SMALLWOOD, A. (1995): Trace elements in precious and common opals using neutron activation analysis. *J. Radioanal. Nucl. Chem.* **198**, 5-7.
- MCORIST, G.D. & SMALLWOOD, A. (1997): Trace elements in Australian opals using neutron activation analysis. *J. Radioanal. Nucl. Chem.* **223**, 9-15.
- MCORIST, G.D., SMALLWOOD, A. & FARDY, J.J. (1994): Trace elements in Australian opals using neutron activation analysis. *J. Radioanal. Nucl. Chem.* **185**, 293-303.
- MOTANI, R. (2004): Rulers of the Jurassic Seas. *Scientific American* **14**, 4-11.
- PECOVER, S.R. (1996): A new genetic model for the origin of opal in Cretaceous sediments of the Great Artesian Basin. *Geol. Soc. Aust.* **43**, 450-454 (extended abstr.).
- PEWKLIANG, B., PRING, A. & BRUGGER, J. (2004): Opalisation of fossil bone and wood: clues to the formation of precious opal. In *Regolith 2004* (I.C. Roach, ed.). CRC LEME, 264-268.
- PUTNIS, A. (2002): Mineral replacement reactions: from macroscopic observations to microscopic mechanisms. *Mineral. Mag.* **66**, 689-708.
- ROBERTSON, R.S. & SCOTT, D.C. (1990): *Geology of the Coober Pedy Precious Stones Field: Results of Investigations, 1981-1986*. Geological Survey, Department of Mines and Energy, Adelaide, South Australia.
- RONDEAU, B., FRITSCH, E., GUIRAUD, M. & RENAC, C. (2004): Opals from Slovakia ("Hungarian" opals): a re-assessment of the conditions of formation. *Eur. J. Mineral.* **16**, 789-799.
- SANDERS, J.V. (1964): Color of precious opal. *Nature* **204**, 1151-1153.
- TAYLOR, S.R. & MCLENNAN, S.M. (1985): *The Continental Crust: its composition and Evolution*. Blackwell Scientific Publications, Oxford, U.K.
- TOWNSEND, I.J. (1976): Stratigraphic drilling in the Arckaringa Basin, 1969-1971. *Geol. Surv. S. Aust., Rep. Invest.* **45**.
- TOWNSEND, J. (2007): Perfect conditions, perfect spheres: opal formation in Australia. In *Opal, the Phenomenal Gemstone*. *ExtraLapis* **10**, 18-21.
- WILLIAMS, L.A. & CRERAR, D.A. (1985): Silica diagenesis. II. General mechanisms. *J. Sed. Petrol.* **55**, 312-321.
- WILLIAMS, L.A., PARKS, G.A. & CRERAR, D.A. (1985): Silica diagenesis. I. Solubility controls. *J. Sed. Petrol.* **55**, 301-311.

Received December 5, 2006, revised manuscript accepted October 6, 2007.

